Subfossil Simuliidae track past river flow into an industrially contaminated lake

Brigitte Simmatis[1] (12bsgs@queensu.ca), Alexandre Baud[2] (alexandre.baud@mail.mcgill.ca), Irene Gregory-Eaves[2] (irene.gregory-eaves@mcgill.ca), Pierre Francus[3] (pierre.francus@ete.inrs.ca), and John P. Smol[1] (smolj@queensu.ca)

[1]Paleoecological Environmental Assessment and Research Lab (PEARL), Department of Biology, Queen's University, Kingston, Ontario, K7L 3N6 Canada

[2]Department of Biology, McGill University, Montreal, Québec, H3A 1B1 Canada

[3]Centre Eau Terre Environnement, Institut National de la Recherche Scientifique, Québec City, Québec, G1K 9A9 Canada

Keywords: Black flies, Paleohydrology, Chironomidae, Nuisance algal blooms, Cultural eutrophication

Corresponding author:

Brigitte Simmatis,

Telephone: (613) 888-1571

Email: 12bsgs@queensu.ca

Abstract

Stoco Lake (Tweed, Ontario, Canada) has a history of industrial contamination and is heavily influenced by inflow from the Moira River. Stoco Lake is frequently affected by nuisance algal blooms (including cyanobacteria), which have largely been attributed to cultural eutrophication. To further our understanding of the environmental dynamics of Stoco Lake, we applied paleolimnological techniques to examine long-term trends in subfossil invertebrate assemblages, geochemistry, and inferred trends in whole-lake primary production from a sediment core representing ~70 years of environmental history. We examined past trends in Simuliidae abundance, geochemical variables, and historical river flow records to examine past hydrological conditions in Stoco Lake. Inferred whole-lake primary production and sediment core organic content increased between the late 1950s and early 1970s, likely reflecting increased eutrophication (e.g. from agricultural intensification and increased catchment activities), with some stabilization in the post-1970s sediments coinciding with the installation of a sewage treatment plant. The geochemical composition of the core highlighted the decrease in catchment-derived sediment inputs and an increase in percentage of organic content towards the top of the core. In addition, declines in the proportion of As and Ni coincided with the closure of the upstream Deloro Mine Site in the 1960s. Chironomidae and Chaoboridae (Diptera) assemblages indicate expansion of littoral habitat after the 1960s and a general stability of low-oxygen conditions in the hypolimnion over the past ~70 years. Several Simuliidae (Diptera: Nematocera) remains, indicators of fluvial conditions rarely discussed in paleolimnological studies, were present at their highest abundances in the pre-~1975 sediments of the core, but disappeared after the early 1990s. Our findings suggest that changes in river flow (discharge, velocity, or seasonality) may have contributed to recent algal blooms. Overall, this study highlights the

potential of Simuliidae in paleohydrological studies to help understand the role of river flow on lake conditions.

Introduction

The vast majority of morphologically identifiable remains used in paleolimnological studies are diatoms, cladocerans, and chironomids, as they are common in many lake sediment cores. Only rarely are subfossil invertebrate remains characteristic of lotic environments encountered or identified. Nonetheless, taxa such as Trichoptera, Ephemeroptera, and Simuliidae provide significant insights into long-term changes in aquatic ecosystems (Williams 1988; Howard et al. 2009; Rück et al. 1998).

Simuliidae (Diptera; commonly called black flies, herein referred to as simuliids) larvae are common in unpolluted, flowing waters in North America, with the majority of taxa restricted to lotic habitats (Currie and Walker 1992). However, they are often rare subfossils in lake sediment cores (generally reported as <5% of Dipteran assemblages; Luoto 2010), as flowing waters are not generally conducive to sediment deposition and lake coring sites do not often adequately capture black fly habitats (Currie and Walker 1992). Simuliids have a strong relationship with changes in stream flow and water level (Feld et al. 2002), offering information regarding past hydrology that can be difficult to disentangle with more common invertebrate remains (Currie and Walker 1992). Furthermore, certain simuliid taxa are specialists and can provide more specific paleohydrological information. For example, immature *Stegopterna* are often restricted to small first-order streams, whereas others, such as *Simulium* and *Prosimulium*, are generalists, but can still be informative about overall changes in river influence on lentic environments (Currie and Walker 1992).

Some Chironomidae (Diptera) taxa have also been associated with lotic environments and can be useful for refining information provided by simuliids. For example, *Rheotanytarsus* and *Nanocladius branchiolus*-type subfossils were associated with running waters in a Finnish intralake calibration set (Luoto 2010). Chironomid subfossil assemblages, however, are more often used to reconstruct temperature (Walker 2001; Walker et al. 1997) or late-summer hypolimnetic oxygen conditions (Quinlan and Smol 2001a; Quinlan et al. 1998).

We explored how simuliid assemblages can be used to interpret changes in river inflow within a paleohydrological context. We examined the midge (Diptera: Chironomidae and Chaoboridae, herein referred to as chironomids and chaoborids, respectively) and simuliid assemblages in a ~70-year lake sediment record from Stoco Lake near Tweed, Ontario, Canada. In addition, we applied a multi-proxy approach to further our understanding of the environmental dynamics of a lake that has experienced multiple environmental stressors. The goals of this study were to determine whether Simuliidae reflect changes in past river flow, to evaluate if changes in primary production may be linked to changes in river flow, and to more broadly reconstruct the environmental dynamics of Stoco Lake.

Site description

Stoco Lake (44.47° N, 77.29° W; Fig. 1) is a relatively shallow ($z_{max} = 11$ m, $z_{mean} = 4$ m), small (SA = 0.53 km^2) lake with two basins. The regional landscape includes drumlin and esker formations, a granite-limestone transitional zone, and many commercially viable mineral deposits (e.g. gold, silver, actinolite, marl, and marble; SLSP 2017). Much of the watershed is on Precambrian Shield bedrock with poorly developed soils and thin tills. Agricultural activities are most prevalent in areas with limestone bedrock and on isolated pockets of suitable soils on the Shield, including areas in close proximity to Stoco Lake (Quinte Conservation 2008; Fig. 1). Analyses of mean annual temperature data from the closest weather station at Belleville, ~40 km south of Tweed, show an overall increasing trend (Fig. 1b).

The water chemistry in Stoco Lake is dominated by the flow from the major tributary of the Moira River (MOE 1984). The lake watershed, including Moira River, Sulphide Creek and Clare River, has an area of approximately 2230 km^2. The lake has a very rapid flushing rate, last estimated in 1984 to occur ~50 times/year (MOE 2012). There are three water control structures located in close proximity to Stoco Lake: Chapman's Weir (West Channel outlet; seasonal installation), Canton's Weir (East Channel outlet; seasonal installation), and a private dam located just downstream of where Bridge Street East (Tweed, Ontario) crosses the Moira River (upstream of Stoco Lake). Historically, Stoco Lake experienced weak dimictic stratification in the deeper southern basin during the 1984 sampling season (MOE 2012) and fall mixing had occurred by early September (MOE 1984, 2012). In summer 2011 (MOE 2012) and in the July 2017 *LakePulse* (Huot et al. 2019) field season, the lake was thermally stratified and had a relatively warm hypolimnion of 13-14°C. Recent (2011) lake water measurements indicate that the lake is alkaline (pH 7.9) and mesotrophic (epilimnetic TP_{May} = 14.5 µg/L), with a Secchi depth of 2.4 m (MOE 2012). In July 2017, the lake had low $TKN_{epilimnetic}$ (0.25 µg/L) and high Ca^{2+} concentrations (31.86 mg/L). In the 2011 sampling year, the surficial lake sediments from the mouth of the Moira River and deepest point had elevated metal concentrations (i.e. As, Ni, Cu, and Co), likely due to the former Deloro Mine Site (which processed primarily Au, As, Ni, and Co between 1860 and 1962), located ~35 km upstream (Mudroch and Capobianco 1980; MOE 2012).

Materials and methods

Core collection and chronology

A 29-cm core was retrieved from 9 m water depth in the main basin of Stoco Lake (Fig. 1a) in July 2017 using an Aquatic Resource Instruments gravity corer (internal diameter of 6.8 cm) and shipped to Université Laval, Québec City, Canada, where it was split vertically. One half of the core was sectioned at 1-cm intervals in the lab and subsamples were frozen at -20 °C prior to shipment to Queen's University, Ontario, for further analyses. Following Schelske et al. (1994), freeze-dried sediments from 12 intervals were measured for ^{210}Pb and ^{137}Cs radioisotope activities by gamma spectroscopy, at the Paleoecological Environmental Assessment and Research Laboratory (PEARL). A ^{210}Pb core chronology was established by applying the constant rate of supply (CRS) model (Appleby and Oldfield 1978). ^{137}Cs was used as an independent chronological marker for the 1963 peak of atmospheric nuclear weapons testing.

CT scan and μ-XRF elemental analysis

Prior to any sample processing, the entire core was scanned through a Siemens SOMATOM Definition AS+ 128 computed-tomography (CT) core scanner at the Institut National de la Recherche Scientifique (INRS) in Québec City, Canada. Acquisition parameters were as follows: kV: 140, mAs: 300, rotation time: 1000 ms, pitch: 0.55, collimation: 128 x 0.6 mm, and reconstruction filter: H60 s. CT-scanners measure the attenuation of X-rays that penetrate material and store this information in pixels as relative gray scale values or Hounsfield units (HUs; Hounsfield 1980) in a succession of 2D images in DICOM format, corresponding to 0.6-mm slices perpendicular to the core length. HU values were extracted using a plug-in available in the OsirixLite software (Rosset et al. 2004), by propagating a circular section of 20 cm^2, centered in the middle of each sediment slice (integrating >70% of the sedimentary material found within each DICOM) across the length of the sediment core. Once extracted and compiled, the mean HU value for each slice was calculated and plotted along the sedimentary sequence.

The split sediment core was scanned on a non-destructive Cox Analytics micro-X-ray Fluorescence (μ-XRF) ITRAX core scanner located at INRS. The instrument exposes the core material to X-rays that produce photons with energies specific to each element, then detects and expresses these as counts per unit time per unit area (hereafter cps; Croudace et al. 2006), providing a measure of the relative elemental composition of the sediment core. The core was scanned using a molybdenum-anode X-ray tube at 40 kV and 10 mA at 0.1-mm resolution for 20 s per interval. The *sum spectra* was then re-evaluated using *QSpec*, the proprietary software of the ITRAX, to batch re-evaluate each of the 286 spectra generated by the instrument.

VRS-inferred chlorophyll *a*

Visible range spectroscopy (VRS) can track trends in whole lake primary production by inferring the concentration of sedimentary chlorophyll *a* (along with its isomers and main degradation products), providing information on shifts in lake trophic status (Michelutti and Smol 2016; Michelutti et al. 2010). Sediments were processed using standard methods (Wolfe et al. 2006; Michelutti et al. 2010). In short, freeze-dried sediments were sieved through a 125-µm screen to remove coarse grain sizes, then analyzed using a FOSS NIRSystem Model 6500 Rapid Content Analyzer, operating over a range of 400 – 2500 nm. Trends in the concentration of chlorophyll *a* and its diagenetic products were inferred from spectral absorbance values in the 650 – 700 nm wavelength range, using a linear model (Wolfe et al. 2006; Michelutti et al. 2010).

Invertebrate preparation and identification

Chironomid, chaoborid, and simuliid remains were prepared using standard methods (Walker 2001). Briefly, subsampled sediments were heated at ~80 °C in 5% KOH for 20 minutes. Samples were rinsed over a 100-μm sieve with deionized water to remove smaller particles of sediment, then concentrated into a glass beaker. The entirety of each beaker was examined using a Leica dissecting microscope at 32× magnification. Chironomid head capsules, chaoborid mandibles, and simuliid hypostomes were manually transferred onto cover slips with fine forceps and permanently mounted to microscope slides using Entellen®. At least 40-50 whole chironomid head capsules (Quinlan and Smol 2001b) were identified to the lowest possible taxonomic level in each sediment interval using a Leica DMZ500 microscope with brightfield illumination and referencing Brooks et al. (2007) and Anderson et al. (2013). Chaoborid mandibles were also isolated and identified using Uutala (1990) as the primary reference.

Subfossil simuliid remains (Fig. 2) appear superficially similar to chironomid head capsules in size and structure (Luoto 2010; Walker 2001; Currie and Walker 1992). Entire head capsules or fragmented ventral structures with hypostomal teeth (roughly equivalent to chironomid menta) can be recovered and are identifiable to at least the genus level (Currie and Walker 1992). Frontoclypeal apotomes are somewhat more common than the head capsule itself, but offer less diagnostic information. Simuliid hypostomes were identified to the genus level following Currie and Walker (1992). All the simuliid remains found were fully intact hypostomes, but lacked the frontoclypeal apotomes, and each hypostome was counted as one individual or the equivalent of one whole chironomid mentum.

Statistical methods

A principal component analysis was performed on the chironomid data using the “vegan” package in R (Oksanen et al. 2017) to determine if there were directional temporal trends in the assemblages. Elemental relative abundances were standardized using total cps (expressed in thousands of counts per second) and density (inferred from HU values; Kenter 1989) estimates for each 1-mm integration. Standardized counts were then plotted as elements and data were modelled using generalised additive models (GAMs) in R to highlight trends. For all GAMs, Gaussian models were fit using cubic basis splines and analyses were performed in R using the “mgcv” and “Hmisc” packages.

Results

Core chronology

^{210}Pb activities approximately followed an exponential decay curve with core depth, but only the basal two samples showed overlap between ^{214}Pb and ^{210}Pb activities when error bars were considered (Fig. 3A). ^{137}Cs activities rose up-core, then fell, displaying a gradual peak around ~15 cm (Fig. 3A).

The initial chronology produced by ScienTISSiMe software estimated a basal date of ca. 1756. However, the profile violated the “Binford Rule,” defined as having three unsupported ^{210}Pb activity measurements with the mean and one standard deviation less than the supported

^{210}Pb activity (estimated by ^{214}Pb in this study; Binford 1990). Furthermore, the CRS model had a consistently poor fit between estimated activities compared to the measured activities throughout the sediment core, with a low r^2 value and generally scattered estimated activities, likely because the initial model set the three bottom-most intervals as "background," despite the fact that some intervals had non-zero activities greater than the unsupported values. Both As and Ni showed elevated concentrations in the deepest sediments that declined at ~20 cm. Given that upstream mining began in 1867, it is unlikely we would observe no apparent increase in As or Ni with the start of operations if the basal date were truly pre-1860. Modern monitoring and previous studies have also shown that the contamination from the Deloro Mine Site does reach Stoco Lake, even at levels that could be harmful to benthic invertebrates (e.g. MOECC 2011). We also examined the chronology of another dated sediment core from Moira Lake (Tenkouano et al. 2019), approximately 20 km upstream from Stoco Lake on the Moira River. Moira Lake has a longer water residence time and is less productive than Stoco Lake. Peaks in As, Co and Ni occurred between 30 cm and 20 cm (in the 1930s-1950s) in this Moira Lake core (Tenkouano et al. 2019). The 50-cm sediment core from Tenkouano et al. (2019) had a basal date of ca. 1790, also indicating relatively high sedimentation rates in the region. We were therefore skeptical of a pre-1860 basal date for several reasons and re-ran the age model with different assumptions.

We developed Stoco Lake's chronology using the activity from the 28.5-cm stratum as the "background" supported ^{210}Pb activity in ScienTISSiMe, since this was just less than the measured ^{214}Pb (supported ^{210}Pb) profile. Using this depth for the unsupported/supported ^{210}Pb boundary, the adjusted CRS model yielded a basal date of ca. 1950. Although a record of this length provides adequate information to assess the potential recent recovery of Stoco Lake from eutrophication, it does not capture the pre-impact period (i.e. initial land clearance, regional mining activity or onset of cultural eutrophication).

Invertebrate assemblages

In total, 1379 whole chironomid head capsules from 36 taxa were recovered from 26 sediment intervals. Taxa present at >5% relative abundance in at least two intervals were plotted stratigraphically (Fig. 4). There were no distinct unidirectional trends evident in axes 1 or 2 of the downcore principal component analysis (Figs. 5a, b), and the inertia was quite even across the first five axes. Taxonomic changes in the chironomid assemblage were generally subtle, though trends in other components of the assemblage were less stable, including head capsule concentration (Fig. 5d), the ratio of littoral to profundal taxa (Fig. 5e), and the relative abundance of Simuliidae in the sediment record (Fig. 5g). The concentration of chironomid head capsules (HC) increased through time, reaching a maximum of 246 HC/g dry sediment weight in strata corresponding to ~1980s (7.5 cm; Fig. 5d). The flux of head capsules also increased after ca. 1990 (6 cm; Fig. 5d). The average ratio of littoral and profundal chironomid taxa was ~2.1 throughout the core, indicating that the chironomid assemblages were primarily composed of littoral taxa (Fig. 5e).

The most common taxon was *Tanytarsus*, with a ~25% mean relative abundance (42% maximum relative abundance; Fig. 4). Macrophyte-associated taxa, including *Labrundinia*, *Dicrotendipes*, and *Glyptotendipes*, were present at lower relative abundances (~5-15%). *Procladius* was the second most common taxon (~30% relative abundance) until ca. 1958 (18 cm), but then dropped to 15-20%, when *Tanytarsus* became dominant (25-30%; Fig. 5). Subdominant taxa (*Sergentia*, *Micropsectra* and *Chironomus*) did not show any clear temporal trends. Semi-aquatic or lotic taxa, such as *Chaetocladius* and *Smittia-Parasmittia* (each at ~10% abundance), were relatively stable through time (Brooks et al. 2007; Fig. 4). Likewise, Chaoborid remains were distributed relatively evenly throughout the core (Fig. 5f; a total of 263 *Chaoborus* mandibles were recovered throughout the whole record). *Chaoborus* assemblages were composed of primarily *C. (Sayomyia)*-type mandibles, with a small proportion of the chaoborid assemblage composed of *C. flavicans*.

In total, 33 simuliid hypostomes were found, primarily in older (pre-ca. 1993; >5 cm) sediments. The simuliid assemblage was composed of *Simulium* and *Prosimulium*. A maximum of 7 hypostomes were recovered in any one interval and reached 11% of the dipteran assemblage in the 17-18 cm sediment interval (corresponding to ca. 1959; Fig. 5g).

VRS-inferred trends in chlorophyll *a*

In the late-1960s, VRS-inferred chlorophyll *a* (which includes its main diagenetic products) began to increase, doubling in concentration between ca. 1957 (19 cm) and ca. 1970 (10 cm; Fig. 5c). After ca. 1970, trends in VRS-inferred chlorophyll *a* continued to increase to the top of the core, but at a slower rate (Fig. 5c).

µ-XRF elemental analysis and CT scan results

GAMs were fit to represent overall trends in the data and performed well (k = 20, r^2_{adj} varied from 0.67 for As to 0.99 for density; Fig. 6). A decline in the density of the sediments was apparent in the profile (Fig. 6a), and was matched by an increasing trend in the ratio of inelastic Compton scattering (Inc) and the elastic Rayleigh scattering (Coh; Fig. 6b), which is an indicator of organic content and water content in the sediment core (referred to as Inc:Coh; Croudace and Rothwell 2015). The elemental profile for Titanium (Ti), a marker of terrigenous input (i.e. erosion) in lake sediments (Croudace and Rothwell 2015), displayed a steady decrease throughout the core (Fig. 6c). To determine whether compaction explained the trend in the Ti profile, Ti:Inc was also examined and determined to be decreasing up-core only slightly (Electronic Supplementary Material (ESM] Fig. S1a). Profiles for arsenic (As) and nickel (Ni) revealed a lower relative abundance of these metals in the top of the sediment core relative to the bottom (Fig. 6d, e). There also was a peak in As relative abundance at ca. 1960 (15 cm; Fig. 6d).

Discussion

Stoco Lake, like many lakes in the southern temperate zone of the Canadian landscape, has experienced multiple stressors over the last century. Our paleolimnological record provides insight into how a weakly dimictic, fast-flushing lake with upstream mining activity, as well as nutrient abatement and climate change, varied over a ~70-year period. Due to the relatively fast sedimentation rates, the 29-cm sediment core did not capture European settlement and had an estimated basal date of ca. 1950. The relatively high ^{210}Pb activities in the older part of the core compared to the supported activities, elevated metal concentrations (As and Ni) at the base of the sediment core, and the gradual, relatively deep peak in ^{137}Cs support our dating model results. Although it is possible that ^{137}Cs may be somewhat mobile in organic sediments (Crusius and Anderson 1995; Comans et al. 1989), there was very low ^{137}Cs activity in the most organic-rich sediments, which span the top 10 cm. It is likely that the high sedimentation rate is related to the strong influence on Stoco Lake of the Moira River, which flushes the lake 50 times per year. The flow from the Moira River may have been more influential in the past, given the decline of Simuliidae taxa in the recent part of the sediment record.

Lotic taxa in the sediment record

Lotic taxa, including Simuliidae, were present in the dipteran assemblages. The influence of the Moira River may have changed over time, resulting in some variation in the midge and simuliid assemblages of Stoco Lake. Unfortunately, discharge rates of the Moira River at Tweed have been measured infrequently since 1972, but consistently since 2003 (Fig. 7a; Government of Canada 2019). Based on monitoring records, spring discharge is peaking earlier in the year than it did in the 1970s. A longer record from Foxboro, Ontario (~40 km downstream from Stoco Lake; Government of Canada 2019) also supports the notion that discharge is peaking earlier in the year than in the past (Fig. 7b). Earlier spring freshet or increased water temperatures could alter the reproductive success, brood or population size, emergence and/or voltinism regimes of Simuliidae (Colbo and Porter 1981; Singh and Smith 1985).

The substantial numbers of Simuliidae subfossils is relatively unusual in lake sediment records, as they are typically found only in flowing waters (Currie and Walker 1992). In particular, Simuliidae larvae can often be found in the flowing waters of lake outlets, feeding primarily on seston (Richardson and Mackay 1991). Simuliidae are uni-, bi-, or multivoltine, depending on the species (Currie and Walker 1992). Though primarily filter feeders, Simuliidae can supplement their diet by scraping organic material from the substrates to which they are attached, using a pad of salivary secretions or silk (Currie and Walker 1992). Several authors have suggested that changes in Simuliidae assemblages can be used to infer past hydrological conditions (Currie and Walker 1992; Luoto 2010), but often Simuliidae make up only a small proportion of midge assemblages in profundal lake sediment cores (i.e. <5%; Luoto 2010).

In Stoco Lake, simuliids were present to a maximum relative abundance of 11% when the entire midge assemblage (chironomids + chaoborids + Simuliidae) was considered, but disappeared from the record in the most recent sediments, estimated to be after ca. 1990. The Ti profile, which was previously used to infer detrital input (Dunnington et al. 2018) or silt (Cuven et al. 2010) content, provides corroborating, but indirect support for diminished stream flow, as heavier particles are only transported by fast-flowing waters. Furthermore, the majority of the Ti profile is not fully explained by a compaction-only signal (ESM Fig. S1), indicating that there may have been a decline in detrital or silt input over time. Decreased local erosion or cultural eutrophication are alternative hypotheses that could explain the decline in Ti, but these would not necessarily explain the complete disappearance of Simuliidae.

In general, the chironomid assemblages in the Stoco Lake record have been relatively stable through time, with the gradual transition from a *Procladius*-dominant to *Tanytarsus*-dominant community in the middle of the sediment record (ca. the 1970s) as the most notable change. The increase in primarily littoral generalists like *Tanytarsus* spp. could reflect an expansion of littoral habitat, which can occur with increased primary production from cultural eutrophication (Brodersen and Quinlan 2006) and would be consistent with the trends in VRS-inferred chlorophyll *a*. *Chaetocladius* and *Smittia* are typically semi-terrestrial to terrestrial chironomid taxa (Luoto 2011), which could indicate shoreline erosion, riverbank erosion, or water level changes. A combination of frequent spring ice jams, flooding, and wake from boat traffic are other factors that could contribute to the presence of semi-terrestrial taxa to the Stoco Lake sediment record. Finally, the chaoborid and profundal chironomid assemblages indicate generally stable and low deep-water oxygen conditions (Quinlan and Smol 2001a, 2010), with the exception of *Micropsectra*, which is typically found in well-oxygenated hypolimnia (Quinlan and Smol 2001a; Brodersen et al. 2008). *Micropsectra* (especially *M. radialis*), however, is a stronger indicator of hypolimnetic oxygen conditions when recorded at >10% relative abundance (Quinlan and Smol 2001a; Brodersen and Quinlan 2006). The presence of *Micropsectra* in the Stoco Lake record may be attributable to winter colonization, when conditions are temporarily suitable for larval survival (Brodersen and Quinlan 2006), or may be sourced from local river environments.

Inferred trends in primary production and river influence

Inc:Coh and VRS-inferred chlorophyll *a* profiles show similar patterns through time. The organic content and whole-lake primary production indicators were initially low and stable for ~10 cm at the base of the core (until ca. 1955), and then increased and reached a new equilibrium starting around the time of the transition from *Procladius*-dominant assemblages to *Tanytarsus*-

dominated assemblages (ca. the 1970s). The most variable period was between ca. 1960 and ca. 1975, which was just prior to the installation of a sewage treatment plant on the Moira River near Tweed.

A combination of μ-XRF elemental analyses and VRS-inferred chlorophyll *a* was examined to determine whether changes in erosional indicators (such as Ti) could support reduced river flow and therefore the trends observed in the dipteran assemblages. The inferred increases in whole-lake primary production and μ-XRF-inferred sediment organic content may be related to a combination of diffuse sources (e.g. agricultural intensification, artificial fertilizers) and point sources (e.g. population growth). Declines in Ti and density, in combination with increases in Inc:Coh (though this may also be linked to water content) in the Stoco Lake sediment core, would support decreased watershed erosion and could also partially reflect higher organic content in the sediment. Changes in the seasonality of river discharge (Fig. 7) appear to have occurred over the period covered by the sediment record, which could have altered the sedimentation rate. Finally, the installation of a sewage treatment plant along the Moira River would have reduced external nutrient loading by diverting raw sewage inputs, and could explain slower increases in VRS-inferred chlorophyll *a* in more recent sediments (after ca. 1975). The maintenance of high whole-lake primary production in the most recent sediments (after ca. 1980) could be related to changes in external nutrient sources, climate (Carvalho and Kirika 2003), and/or internal nutrient cycling (Burger et al. 2008). Whereas some trends in the chironomid assemblages can be explained by increased littoral habitat and food availability, trends in detrital or erosional input further support reduced river influence over time, coinciding with changes in simuliids.

Conclusions

Increases in inferred whole-lake primary production, declines in inorganic inputs, and potential changes in river flow are the main environmental changes in Stoco Lake. The chironomid assemblages indicate general stability in oxygen conditions throughout the core. Reductions in river flow or other hydrological changes (supported by monitoring records and μ-XRF elemental records) appear to be reflected by the disappearance of Simuliidae remains in the most recent sediments, though further work examining how many remains are required to adequately characterize changes in Simuliidae assemblages is required. Overall, this study highlights the importance of understanding simuliid paleoecology, assessing current knowledge gaps, and exploring how this information could be applied in future studies.

Acknowledgments

We thank the Natural Sciences and Engineering Research Council of Canada (NSERC) *LakePulse* Network, field crews, organizers, and those who stored and processed the sediment cores. The authors also thank the NSERC CREATE ABATE program and a team grant from FQRNT for funding this research. Funding from the Canada Research Chair program (JPS, IGE and PF) and a scholarship from FQRNT to AB are also acknowledged. We also thank the Eastern Regional Office and Technical Support Section of the Ontario Ministry of Environment, Conservation, and Parks (Mr. Victor Castro and Ms. Laurel Rudd) for providing water quality data, reports, and information. Finally, we thank the two anonymous reviewers who provided constructive feedback and improved the quality of the manuscript.

References

Andersen T, Cranston PS, Epler JH (2013) The larvae of Chironomidae (Diptera) of the Holarctic Region – keys and diagnoses. Insect Syst Evol, Supplement 66: 1-571

Appleby PG, Oldfield F (1978) The calculation of lead-210 dates assuming a constant rate of supply of unsupported ^{210}Pb to the sediment. Catena 5: 1-8

Binford MW (1990) Calculation and uncertainty analysis of ^{210}Pb dates for PIRLA project lake sediment cores. J Paleolimnol 3: 253-267

Brodersen KP, Pedersen O, Walker IR, Jensen M (2008) Respiration of midges (Diperta: Chironomidae) in British Columbian lakes: oxy-regulation, temperature and their role as palaeo-indicators. Freshw Biol 53: 593-602

Brodersen KP, Quinlan R (2006) Midges as paleoindicators of lake production, eutrophication and hypolimnetic oxygen. Quat Sci Rev 25: 1995-2012

Brooks SJ, Langdon PG, Heiri O (2007) The identification and use of Paleoarctic Chironomidae larvae in palaeoecology. Technical Guide No. 10, Quaternary Research Association, London

Burger DF, Hamilton DP, Pilditch CA (2008) Modelling the relative importance of internal and external nutrient loads on water column nutrient concentrations and phytoplankton biomass in a shallow polymictic lake. Ecol Model 211: 411-423

Carvalho L, Kirika A (2003) Changes in shallow lake functioning: response to climate change and nutrient reduction. Hydrobiologia 506-509: 789-796

Colbo MH, Porter GN (1981) The interaction of rearing temperature and food supply on the life history of two species of Simuliidae (Diptera). Can J Zool 59: 158-163

Comans RNJ, Middelburg JJ, Zonderhuis J, Woittiez JRW, de Lange GJ, Das HA, van der Weijden CH (1989) Mobilization of radiocaesium in pore water of lake sediments. Nature 339: 367-369

Croudace IW, Rindby A, Rothwell RG (2006). ITRAX: Description and evaluation of a new multi-function X-ray core scanner. Geological Society, London, Special Publications, 267: 51-63

Croudace IW, Rothwell RG (Eds.) (2015) Micro-XRF Studies of Sediment Cores: Applications of a non-destructive tool for the environmental sciences (Vol. 17). Springer, Dordrecht, Netherlands

Crusius J, Anderson RF (1995) Evaluating the mobility of ^{137}Cs, $^{239+240}$Pu and ^{210}Pb from their distributions in laminated lake sediments. J Paleolimnol 13: 119-141

Currie DC, Walker IR (1992) Recognition and paleohydrologic significance of fossil black fly larvae with a key to Nearctic genera (Diptera: Simuliidae). J Paleolimnol 7: 37-54

Cuven S, Francus P, Lamoureux SF (2010) Estimation of grain size variability with micro X-ray fluorescence in laminated lacustrine sediments, Cape Bounty, Canadian High Arctic. J Paleolimnol 44: 803-817

Dunnington DW, Spooner IS, Krkošek WH, Gagnon GA, Cornett RJ, Kurek J, White CE, Misiuk B, Tymstra D (2018) Anthropogenic activity in the Halifax region, Nova Scotia, Canada, as recorded by bulk geochemistry of lake sediments. Lake Reserv Manage 34: 334-348

[ECCC] Environment and Climate Change Canada (2019) Monthly data reports (1866-2018): Belleville, Weather ID 6150689; Accessed on 23 May 2019 from http://climate.weather.gc.ca

Feld CK, Kiel E, Lautenschläger M (2002) The indication of morphological degradation of streams and rivers using Simuliidae. Limnologica 32: 273-288

Government of Canada (2019) Historical hydrometric data reports: Moira River near Foxboro (1915-2018, Station ID 02HL001), Moira River at Tweed (1968-1977, Station ID 02HL101), and Moira River near Tweed (2002-2018, Station ID 02HL007); Accessed on 12 July 2019 from https://wateroffice.ec.gc.ca

Horvath TG, Martin KM, Lamberti GA (1999) Effect of zebra mussles, *Dreissena polymorpha*, on macroinvertebrates in a lake-outlet stream. Am Midl Nat 142: 340-347

Hounsfield GN (1980) Computed medical imaging. Med Phys 7: 283-290

Howard LC, Wood PJ, Greenwood MT, Rendell HM (2009) Reconstructing riverine paleo-flow regimes using subfossil insects (Coleoptera and Trichoptera): the application of the LIFE methodology to paleochannel sediments. J Paleolimnol 42: 453-466

Huot Y, Brown CA, Potvin G, Antoniades D, Baulch HM, Beisner BE, Bélanger S, Brazeau S, Cabana H, Cardille JA, Giorgio PA, Gregory-Eaves I, Fortin M-J, Lang AS, Laurion I, Maranger R, Prairie YT, Rusak JA, Segura PA, Siron R, Smol JP, Vinebrooke RD, Walsh DA (2019) The NSERC Canadian Lake Pulse Network: A national assessment of lake health providing science for water management in a changing climate. Sci Total Environ. 695: https://doi.org/10.1016/j.scitotenv.2019.133668

Kenter JAM (1989) Applications of computerized tomography in sedimentology. Mar Georesour Geotec 8: 201-211

Luoto TP (2010) Hydrological change in lakes inferred from midge assemblages through use of an intralake calibration set. Ecol Monographs 80: 303-329

Luoto TP (2011) Indicator value of midge larvae (Diptera: Nematocera) in shallow boreal lakes with a focus on habitat, water quality, and climate. Aquat Insects 33: 351-370

Michelutti N, Blais JM, Cumming BF, Paterson AM, Rühland KM, Wolfe AP, Smol JP (2010) Do spectrally inferred determinations of chlorophyll *a* reflect trends in lake trophic status? J Paleolimnol 143: 205–217

Michelutti N, Smol JP (2016) Visible spectroscopy reliably tracks trends in paleo-production. J Paleolimnol 56: 253-265

[MOE] Ontario Ministry of the Environment and Climate Change (1984) Investigation of Nuisance Algae and Water Quality of Stoco Lake 1984. Accessed on 19 Nov 2017 from http://friendsofstocolake.ca/wp-content/uploads/2015/09/MOE-Stoco-1984-Lake-Water-Quality-1985.pdf

[MOE] Ontario Ministry of the Environment and Climate Change (2012) State of the Lake: Stoco Lake, County of Hastings, 2011. Accessed on 19 Nov 2017 from http://friendsofstocolake.ca/wp-content/uploads/2015/09/2012-Stoco-Lake-Assessment-Report-TSU.pdf

Mudroch A, Capobianco JA (1980) Impact of past mining activities on aquatic sediments in Moira River basin, Ontario. J Great Lakes Res 6: 121-128

Oksanen J, Blanchet FG, Friendly M, Roeland K, Legendre P, O’Hara RB, McGlinn D, Minchin PR, Simpson GL, Solymos P, Stevens MHH, Szoecs E, Wagner H (2017) Vegan: Community Ecology Package. R package version 2.4-2. http://CRAN.R-project.org/package=vegan

Quinlan R, Smol JP (2001a) Chironomid-based inference models for estimating end-of-summer hypolimnetic oxygen from south-central Ontario shield lakes. Freshw Biol 46: 1529-1551

Quinlan R, Smol JP (2001b) Setting minimum head capsule abundance and taxa deletion criteria in chironomid-based inference models. J Paleolimnol 26: 327-342

Quinlan R, Smol JP (2010) The extant *Chaoborus* assemblage can be assessed using subfossil mandibles. Freshw Biol 55: 2458-2467

Quinlan R, Smol JP, Hall RI (1998) Quantitative inferences of past hypolimnetic anoxia in south-central Ontario lakes using fossil midges (Diptera: Chironomidae). Can J Fish Aquat Sci 55: 587-596

Quinte Conservation (2008) Watershed Characterization. Accessed on 25 Sep 2018 from http://quintesourcewater.ca/site/images/stories/pdfs/watershedcharacterization/watershed_characterization_april_2008.pdf

Richardson JS, Mackay RJ (1991) Lake outlets and the distribution of filter feeders: an assessment of hypotheses. Oikos 62: 370-380

Rosset A, Spadola L, Ratib O (2004) OsiriX: An open-source software for navigating in multidimensional DICOM images. J Digit Imaging 17: 205-216

Rück A, Walker IR, Hebda R. (1998) A palaeolimnological study of Tugulnuit Lake, British Columbia, Canada, with special emphasis on river influence as recorded by chironomids in the lake's sediment. J Paleolimnol. 19: 63-75

Schelske CL, Peplow A, Brenner M, Spencer CN (1994) Low-background gamma counting: applications for ^{210}Pb dating of sediments. J Paleolimnol 10: 115-128

Singh MP, Smith SM (1985) Emergence of blackflies (Diptera: Simuliidae) from a small forested stream in Ontario. Hydrobiologia 122: 129-135

[SLSP] Quinte Conservation, Friends of Stoco Lake, and the Municipality of Tweed (2017) "Stoco Lake Stewardship Plan." Accessed on 25 Sep 2018 from http://friendsofstocolake.ca/wp-content/uploads/2017/06/StocoStewardshipPlanJune15-2017.pdf

Tenkuoano G-T, Cumming BF, Jamieson HE (2019) Geochemical and ecological changes within Moira Lake (Ontario, Canada): a legacy of industrial contamination and remediation. Environ Pollut 247: 980-988

Uutala AJ (1990) *Chaoborus* (Diptera: Chaoboridae) mandibles – paleolimnological indicators of the historical status of fish populations in acid-sensitive lakes. J Paleolimnol 4: 139-151

Walker IR (2001) Midges: Chironomidae and related Diptera. In: Smol JP, Birks HJB, Last WM (eds) Tracking Environmental Change Using Lake Sediments – Volume 4: Zoological Indicators. Kluwer Academic Publishers, Dordrecht, Netherlands, pp 43-66

Walker IR, Levesque AJ, Cwynar LC, Lotter AF (1997) An expanded surface-water paleotemperature inference model for use with fossil midges from eastern Canada. J Paleolimnol 18: 165-178

Williams NE (1988) The use of caddisflies (Trichoptera) in palaeoecology. Palaeogeogr Palaeoclimatol Palaeoecol 62: 493-500

Wolfe AP, Vinebrooke RD, Michelitti N, Rivard B, Das B (2006) Experimental calibration of lake-sediment spectral reflectance to chlorophyll *a* concentrations: methodology and paleolimnological validation. J Paleolimnol 36: 91-100

Figure Captions

Fig. 1 Stoco Lake region and climate. **a** Map of Stoco Lake and surrounding area, with shaded areas representing developed (primarily agricultural) land. Water bodies are shaded black and the coring point is marked with a white star. Inset (top): Stoco Lake is the second lake along the Moira River, and is located downstream of the former Deloro Mine Site. Inset (bottom): Location of Stoco Lake in Canada. **b** Annual Belleville (Ontario) temperature over time (station ID 6150689; ECCC 2019). The black dashed line represents the overall trend since ca. 1920, as determined by a general additive model ($r^2_{adj} = 0.339$, $k = 10$). Earlier data were excluded from trend modelling because of a data gap between the 1880s and 1920s. **c** Total precipitation data from Belleville since the 1860s (station ID 6150689; ECCC 2019)

Fig. 2 Simuliidae morphotypes from Stoco Lake. All scale bars represent 50 μm. **a, b** Hypostomes of *Prosimulium.* **c** Hypostomes of *Simulium*

Fig. 3 Sediment core chronology for Stoco Lake. The dotted line indicates the ^{137}Cs peak, an independent marker of the peak in above-ground nuclear weapons testing in 1963. **a** Radioisotope activities in the Stoco Lake sediment core. **b** Date-depth relationship estimated using the constant rate of supply (CRS) model

Fig. 4 Trends in sedimentary chironomid assemblages over time in Stoco Lake. The stratigraphy (left) divides the assemblages into littoral and profundal communities. Chironomid assemblages are expressed as percent abundances relative to the total number of individuals recovered in each interval (i.e. at least 40-50 whole head capsules, except at 2-3 cm, shaded in grey, where only 23 head capsules were recovered; Quinlan and Smol 2001b). Only taxa with a relative abundance of >3% in at least two sediment intervals were plotted

Fig. 5 Summary of inferred chlorophyll *a* and downcore chironomid community trends plotted by estimated dates. **a** Principal component analysis axis 1 (“PC Axis 1”) sample scores for the chironomid assemblage. b Principal component analysis axis 2 (“PC Axis 2”) sample scores for the chironomid assemblage. **c** VRS-inferred chlorophyll *a*, with the black dashed line representing the average concentration over time. **d** Concentration of head capsules (“[HC]”) and flux of head capsules (“HC flux”). **e** Ratio of profundal to littoral chironomid individuals (“Litt:Prof”). **f** Ratio of chaoborid mandibles to chironomid head capsules (calculated as #chaoborid mandibles/(# chaoborid mandibles + chironomid half head capsules); “Chao:Chir”). **g** Abundance of Simuliidae hypostomes relative to the total number of invertebrates

Fig. 6 Summary of physical and geochemical properties from the Stoco Lake sediment core, plotted by core depth. Solid black lines represent smoothed trends calculated from a generalised additive model (k = 20, r^2_{adj} for each model located at the bottom of each figure) and raw data are plotted with grey points. **a** HU values, a proxy for density. **b** Incoherence-coherence (Inc:Coh) ratio profile. **c** Downcore profile of titanium (Ti). **d** Downcore profile of arsenic (As). **e** Downcore profile of nickel (Ni). **f** CT image of the core. **g** Image taken during elemental analysis of split core

Fig. 7 Seasonal discharge (left y-axis) is represented by the stacked columns (Winter = Dec-Feb, Spring = Mar-May, Summer = Jun-Aug, Fall = Sept-Nov) and annual mean river discharge (right y-axis) is represented by white diamond points. Incomplete records (data from <8 months/year were present) were excluded. Data accessed from Government of Canada (2019). **a** Full annual discharge records for the Moira River at Tweed span the intervals 1972-1975 and 2003-2017. **b**

Full annual records for the Moira River at Foxboro (~40 km downstream of Stoco Lake) span from 1916 to 2018. Data accessed from Government of Canada (2019)

Fig. S1 a The ratio between Titanium and Incoherence (Ti:Inc). **b** Percent water in each sediment core interval, determined by freeze-drying sediments

Figures

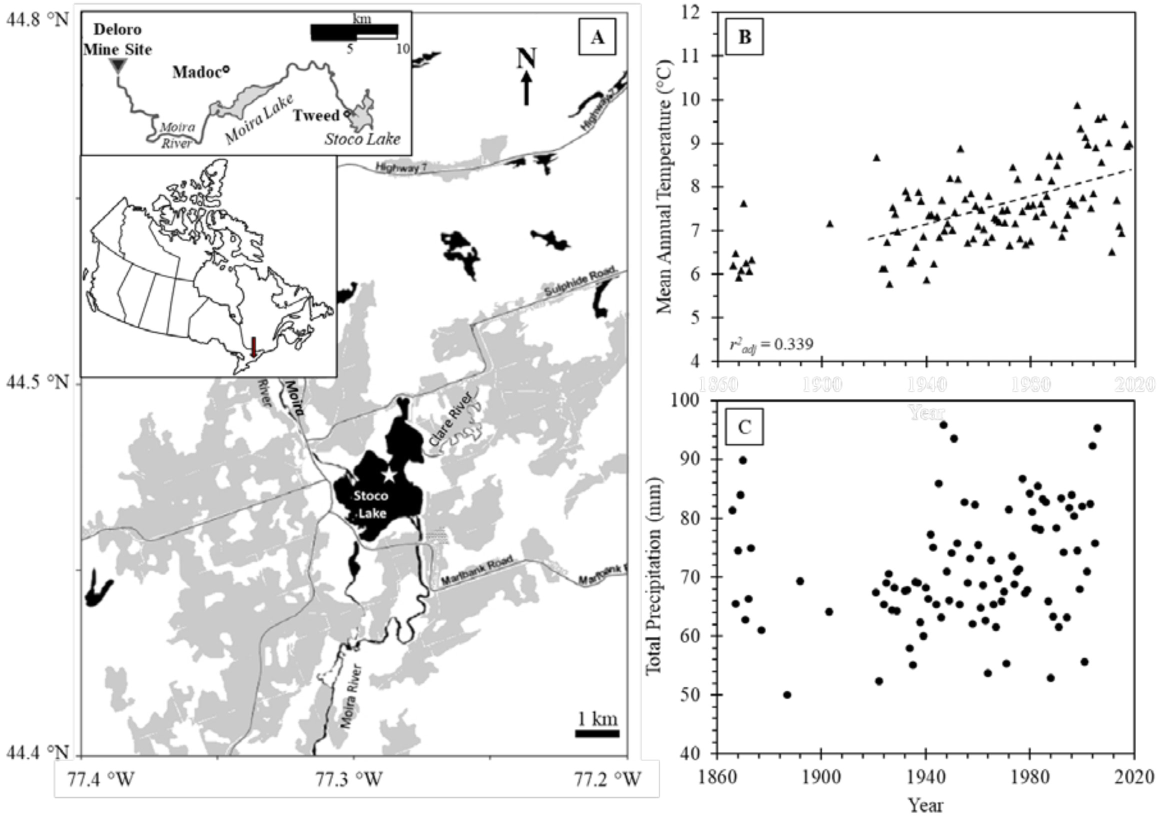
A
B
C
44.8 °N
44.5 °N
44.4 °N
77.4 °W
77.3 °W
77.2 °W
Deloro Mine Site
Madoc
Moira River
Moira Lake
Tweed
Stoco Lake
km
5
10
N
Highway 7
Sulphide Road
Moira River
Clare River
Stoco Lake
Marlbank Road
1 km
Mean Annual Temperature (°C)
r^2_{adj} = 0.339
Total Precipitation (mm)
Year
1860
1900
1940
1980
2020
12
11
10
9
8
7
6
5
4
100
90
80
70
60
50
40

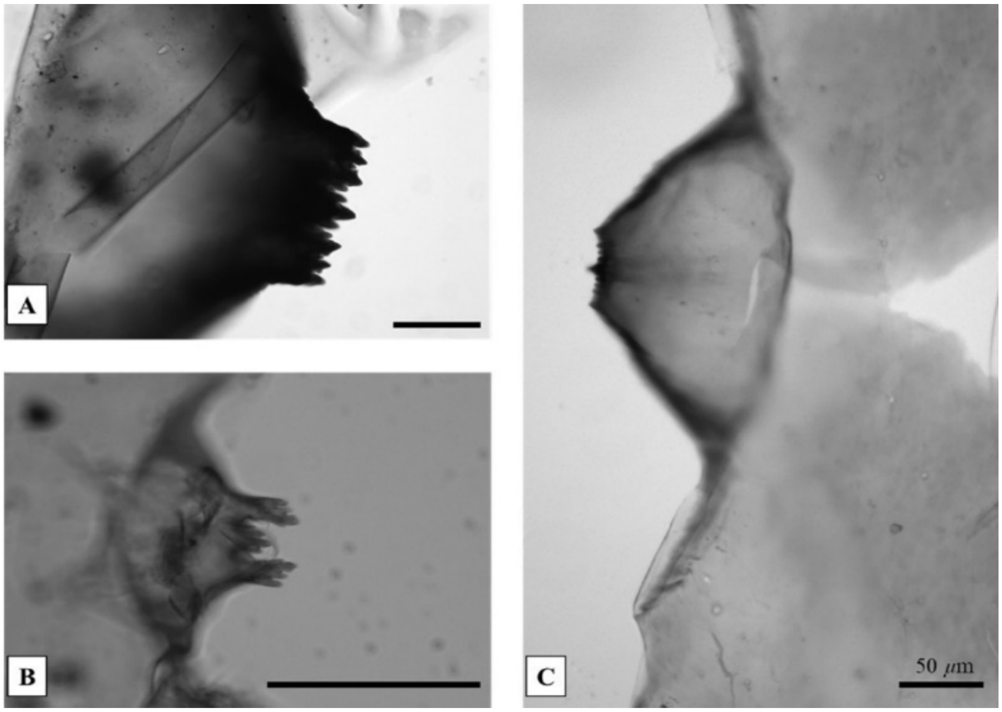
A
B
C
50 μm

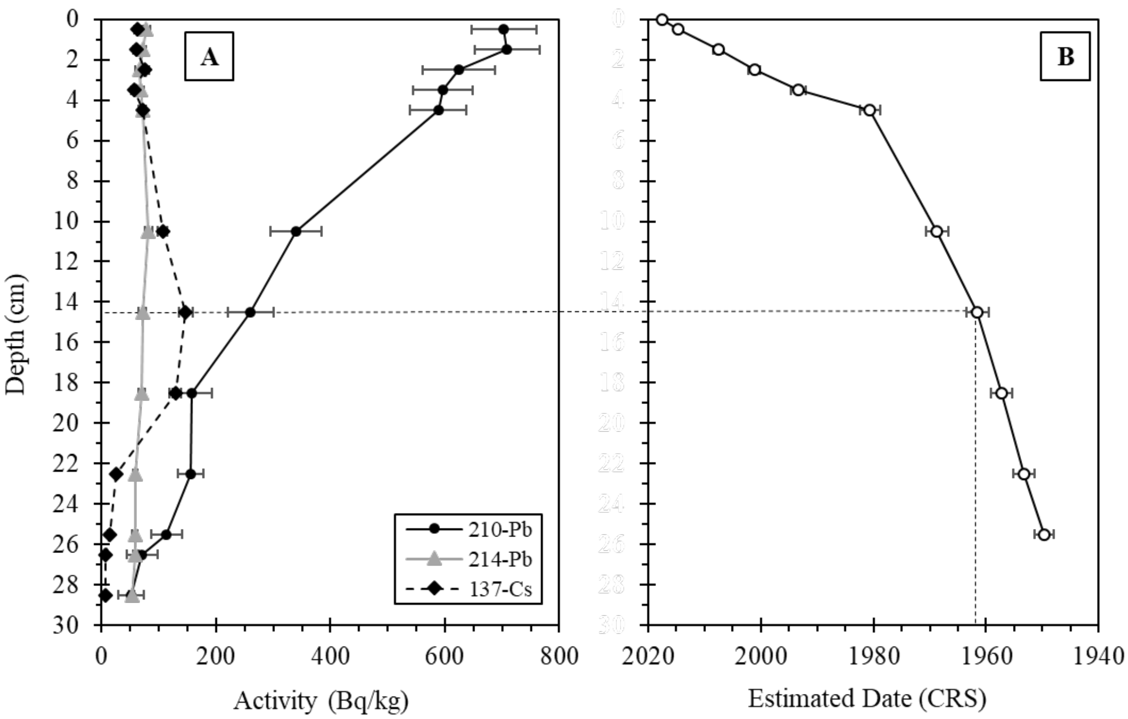
A
B
Depth (cm)
0
2
4
6
8
10
12
14
16
18
20
22
24
26
28
30
0
200
400
600
800
Activity (Bq/kg)
210-Pb
214-Pb
137-Cs
2020
2000
1980
1960
1940
Estimated Date (CRS)

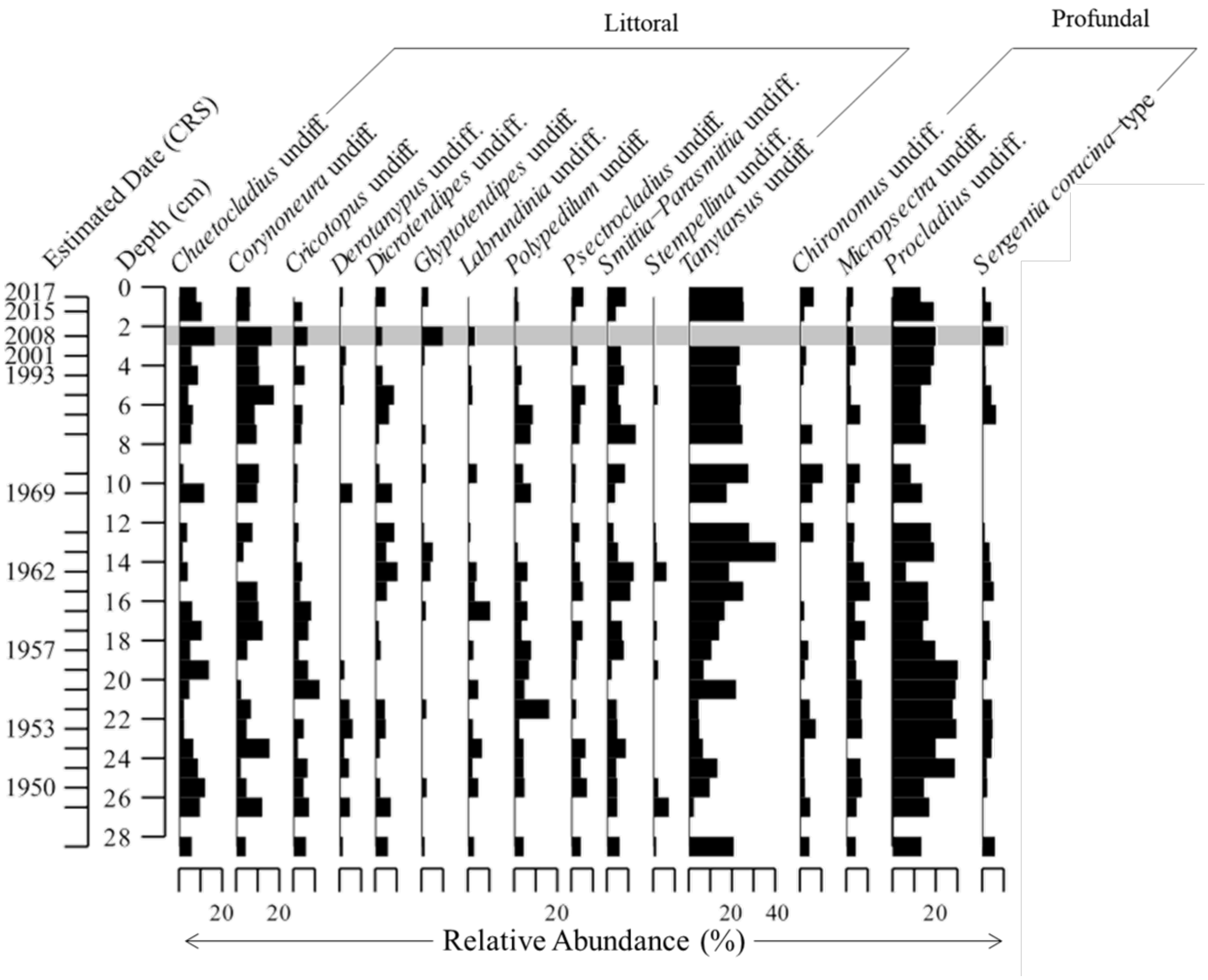
Littoral
Profundal
Estimated Date (CRS)
Depth (cm)
Chaetocladius undiff.
Corynoneura undiff.
Cricotopus undiff.
Derotanypus undiff.
Dicrotendipes undiff.
Glyptotendipes undiff.
Labrundinia undiff.
Polypedilum undiff.
Psectrocladius undiff.
Smittia–Parasmittia undiff.
Stempellina undiff.
Tanytarsus undiff.
Chironomus undiff.
Micropsectra undiff.
Procladius undiff.
Sergentia coracina–type
2017
2015
2008
2001
1993
1969
1962
1957
1953
1950
0
2
4
6
8
10
12
14
16
18
20
22
24
26
28
20
20
20
20
40
20
Relative Abundance (%)

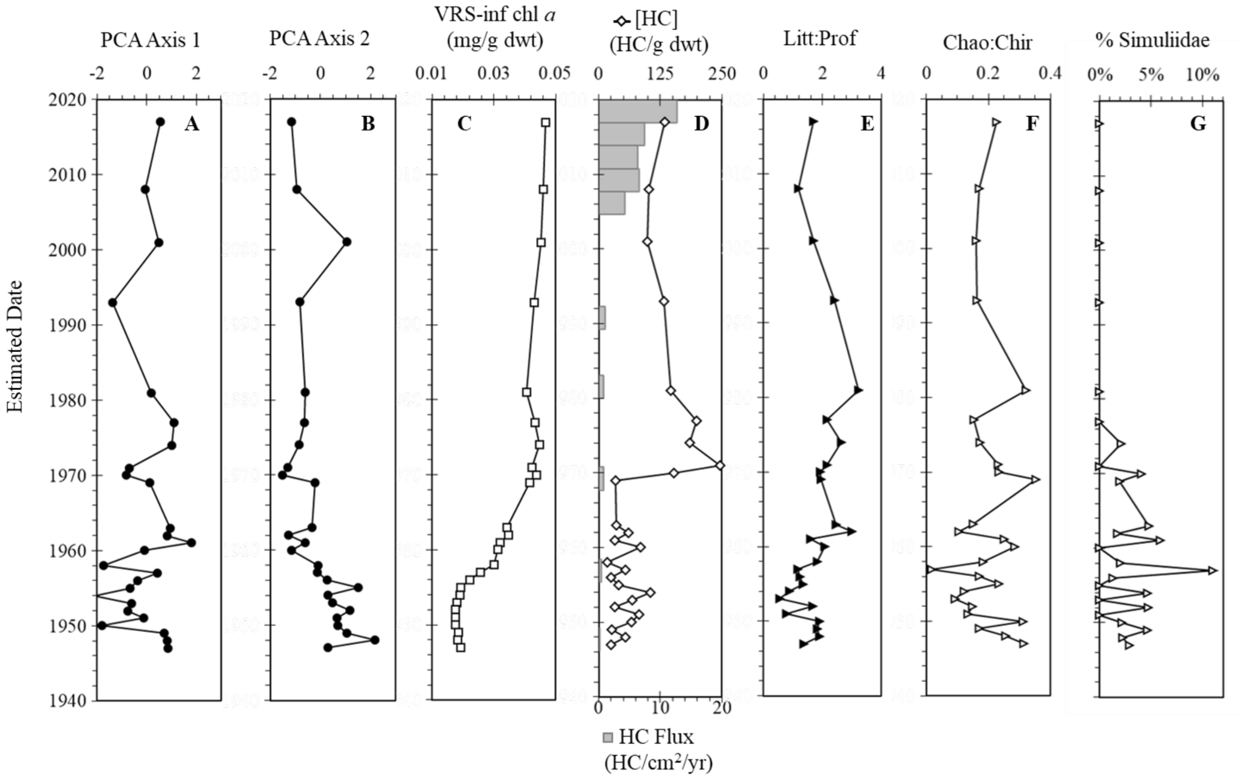
Estimated Date
2020
2010
2000
1990
1980
1970
1960
1950
1940
PCA Axis 1
-2 0 2
A
PCA Axis 2
-2 0 2
B
VRS-inf chl a
(mg/g dwt)
0.01 0.03 0.05
C
◇ [HC]
(HC/g dwt)
0 125 250
D
0 10 20
▨ HC Flux
(HC/cm²/yr)
Litt:Prof
0 2 4
E
Chao:Chir
0 0.2 0.4
F
% Simuliidae
0% 5% 10%
G

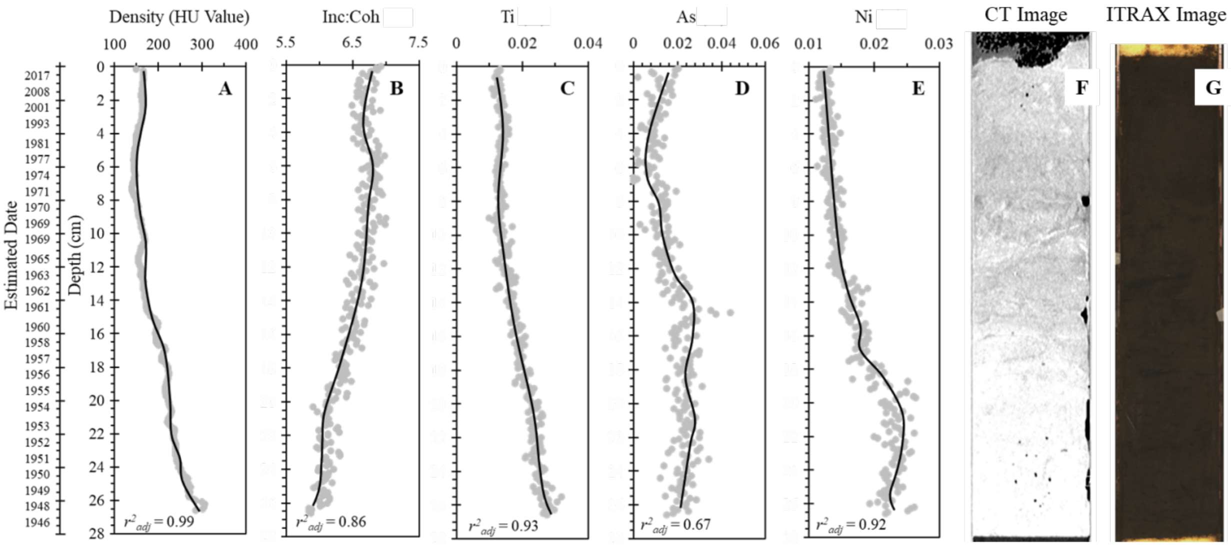
Density (HU Value)
100
200
300
400
Inc:Coh
5.5
6.5
7.5
Ti
0
0.02
0.04
As
0
0.02
0.04
0.06
Ni
0.01
0.02
0.03
CT Image
ITRAX Image
Estimated Date
2017
2008
2001
1993
1981
1977
1974
1971
1970
1969
1969
1965
1963
1962
1961
1960
1958
1957
1956
1955
1954
1953
1952
1951
1950
1949
1948
1946
Depth (cm)
0
2
4
6
8
10
12
14
16
18
20
22
24
26
28
A
B
C
D
E
F
G
$r^2_{adj} = 0.99$
$r^2_{adj} = 0.86$
$r^2_{adj} = 0.93$
$r^2_{adj} = 0.67$
$r^2_{adj} = 0.92$

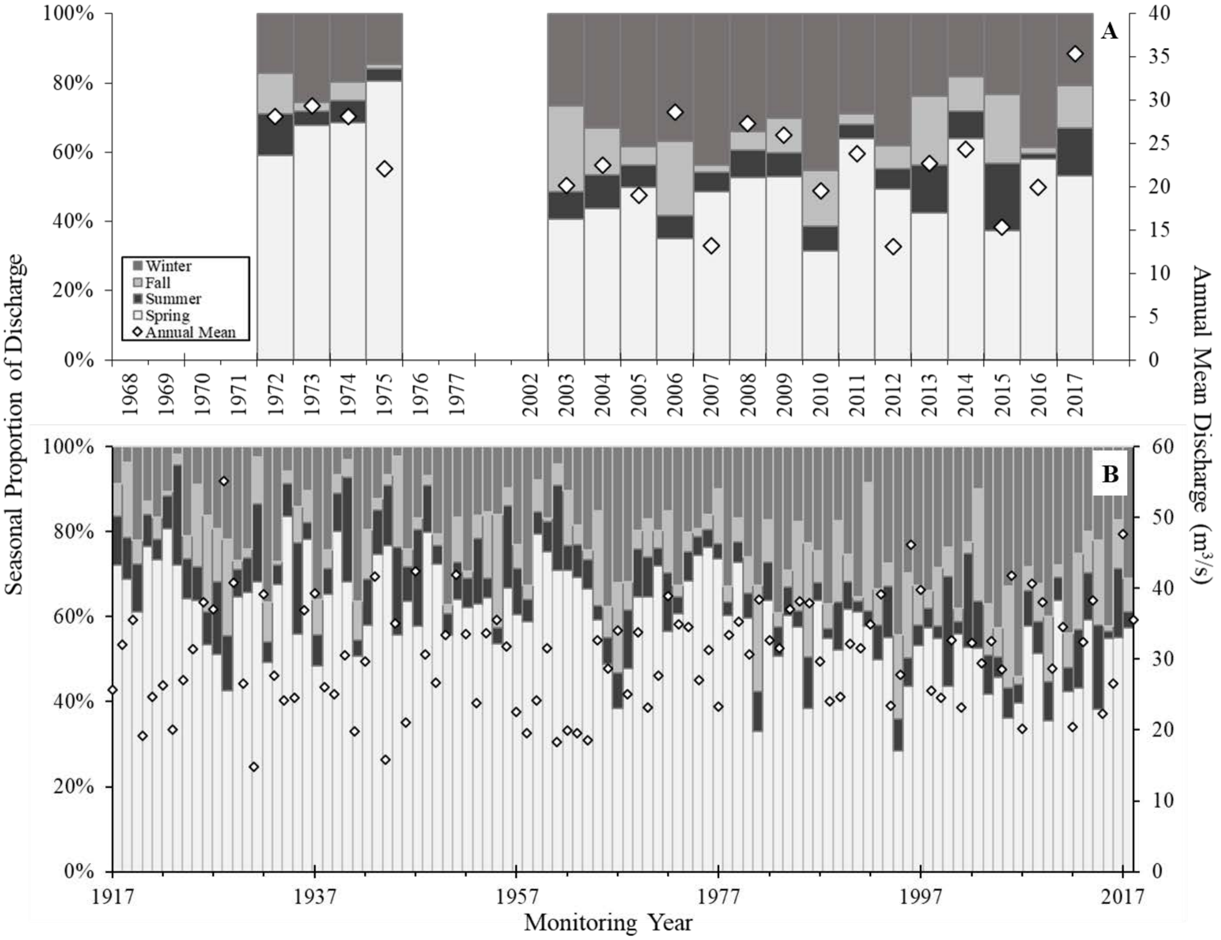
A
B
Winter
Fall
Summer
Spring
Annual Mean
Seasonal Proportion of Discharge
Annual Mean Discharge (m^3/s)
Monitoring Year
100%
80%
60%
40%
20%
0%
40
35
30
25
20
15
10
5
0
60
50
40
30
20
10
0
1968
1969
1970
1971
1972
1973
1974
1975
1976
1977
2002
2003
2004
2005
2006
2007
2008
2009
2010
2011
2012
2013
2014
2015
2016
2017
1917
1937
1957
1977
1997
2017

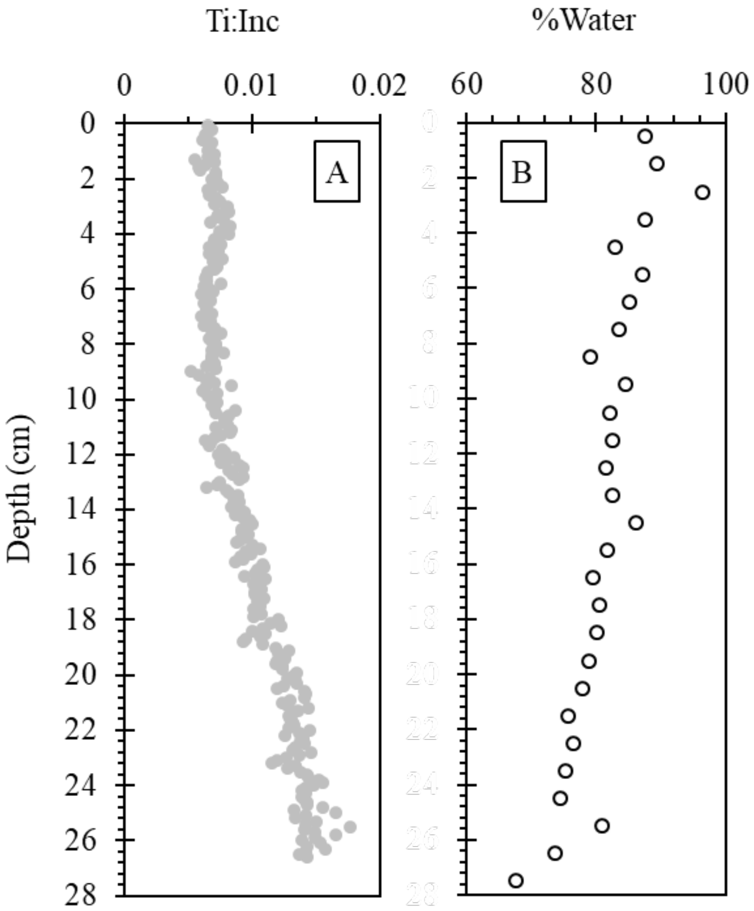
Ti:Inc
%Water
0
0.01
0.02
60
80
100
A
B
Depth (cm)
0
2
4
6
8
10
12
14
16
18
20
22
24
26
28